

CesrTA RETARDING FIELD ANALYZER MEASUREMENTS IN DRIFTS, DIPOLES, QUADRUPOLES AND WIGGLERS*

J.R. Calvey, Y. Li, J.A. Livezey, J. Makita, R.E. Meller, M.A. Palmer,
 R.M. Schwartz, C.R. Strohmman, CLASSE, Cornell University, Ithaca, NY, USA
 K. Harkay, ANL, Argonne, IL, USA[†]
 S. Calatroni, G. Rumolo, CERN, Geneva, Switzerland
 K. Kanazawa, Y. Suetsugu, KEK, Ibaraki, Japan[‡]
 M. Pivi, L. Wang, SLAC, Menlo Park, CA, USA

Abstract

Over the course of the CesrTA program, the Cornell Electron Storage Ring (CESR) has been instrumented with several retarding field analyzers (RFAs), which measure the local density and energy distribution of the electron cloud. These RFAs have been installed in drifts, dipoles, quadrupoles, and wigglers; and data have been taken in a variety of beam conditions and bunch configurations. This paper will provide an overview of these results, and give a preliminary evaluation of the efficacy of cloud mitigation techniques implemented in the instrumented chambers.

INTRODUCTION

The electron cloud is a major limiting factor in the performance of next generation linear collider damping rings. Several mitigation techniques have been proposed to limit the growth of the cloud. Some of these have been tested at CesrTA, including beam pipe coatings[1, 2], clearing electrodes [3], and grooved chambers [4]. Evaluating the efficacy of these methods is an important step in the design of the damping rings.

At CESR, we have installed specially designed RFAs [5] in drift, dipole, quadrupole, and wiggler field regions. RFAs can measure the energy distribution of the cloud by applying a retarding potential between two grids, rejecting any electrons below a certain energy[6]. In addition, most RFAs are segmented across the top of the beam pipe, effectively measuring the transverse distribution of the cloud. We have used these devices to probe the local behavior of the cloud in the presence of different mitigation schemes.

Table 1 provides a list of the mitigation techniques that have been evaluated so far at CesrTA. The italicized items will be discussed in this paper.

DRIFT MEASUREMENTS

Fig. 1 shows a typical retarding voltage scan in an Aluminum drift chamber for a 20 bunch train of positrons, at 2.8 mA/bunch (corresponding to a bunch population of 4.5×10^{10}), 14ns spacing, and beam energy 5.3 GeV. We

* Work supported by the US National Science Foundation (PHY-0734867) and Department of Energy (DE-FC02-08ER41538)

[†] Work supported by the US DoE (DE-AC02-06CH11357)

[‡] Work supported by The Japan/US Cooperation Program

Table 1: Mitigation Techniques at CesrTA

| Field Type | Base Material | Mitigation |
|------------|-------------------------|---|
| Drift | <i>Aluminum, Copper</i> | <i>TiN, Carbon, NEG coatings, solenoids</i> |
| Dipole | <i>Aluminum</i> | <i>TiN coating, grooves</i> |
| Quadrupole | <i>Aluminum</i> | <i>TiN coating</i> |
| Wiggler | <i>Copper</i> | <i>TiN coating, grooves, clearing electrode</i> |

have found these conditions suitable for emphasizing secondary emission, while also allowing for a high total beam current. The plot shows the RFA response as a function of collector number and retarding voltage. The RFA signal is expressed in terms of current density in nA/mm^2 , normalized to the transparency of the RFA beam pipe and grids. In principle, this gives the time averaged electron current density incident on the beam pipe wall. The signal is peaked at low energy and in the central collector, though some current remains at high energy in the central collectors and at low energy in all collectors.

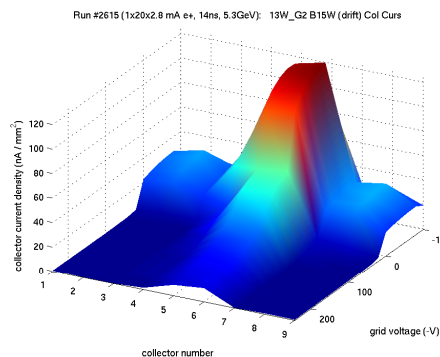


Figure 1: Al drift RFA, 1x20x2.8mA e+, 14ns, 5.3GeV

We have taken RFA data in both TiN and amorphous Carbon coated drift chambers, as well as an uncoated Aluminum chamber. All three of these chambers have been installed at the same location in the ring at different times. This ensures that the comparison is done in the exact same beam conditions, including photon flux and beam size.

A comparison of different beam pipe coatings in a drift region can be found in Fig. 2. It shows the average collec-

tor current density as a function of beam current, for all of the chamber coatings mentioned. There are two sets of data shown for the TiN chamber, one taken shortly after it was installed, and one taken after four months of beam processing. The Carbon chamber has only been installed for a few weeks as of this writing, so a processed Carbon comparison is not yet available.

Both TiN and Carbon coatings show a largely suppressed signal relative to Aluminum, and an approximately equal signal relative to each other. In fact, at the current level of processing, the Carbon chamber falls in between unprocessed and processed TiN.

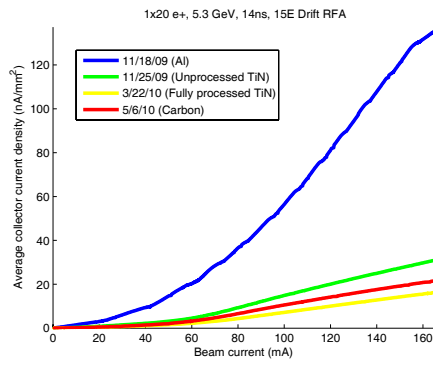


Figure 2: Drift RFA comparison, 1x20 e+, 14ns, 5.3GeV

DIPOLE MEASUREMENTS

Most of our dipole RFA measurements were done using a chicane of four magnets built at SLAC [7]. The field in these magnets is variable, but most of our measurements were done in a nominal dipole field of 810G. Of the four chicane chambers, one is bare Aluminum, two are TiN coated, and one is both grooved and TiN coated. The grooves are triangular with a depth of 5.6mm and an angle of 20°. A retarding voltage scan, done in the Aluminum chamber and with the same beam conditions as Fig. 1, can be seen in Fig. 3. Here one can see a strong central multi-pacting spike, which has actually bifurcated into two peaks with a dip in the middle. This happens when the average energy of electrons in the center of the beam pipe is past the peak of the SEY curve, so that the effective maximum yield is actually off center.

Fig. 4 shows a comparison between three of the chicane RFAs. We found the discrepancy between uncoated and coated chambers to be even stronger than in a drift region. At high beam current, the TiN coated chambers show a signal smaller by a factor of 80 than the bare Al chamber, and the coated and grooved chamber performs better still. Note that the Al signal in these plots is divided by 40.

QUADRUPOLE MEASUREMENTS

A more recent development at CEsrTA is the incorporation of an RFA into a quadrupole chamber. This RFA wraps

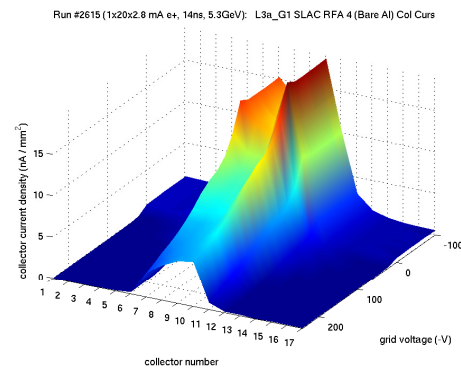


Figure 3: Dipole RFA measurement, 1x20x2.8mA e+, 14ns, 5.3GeV

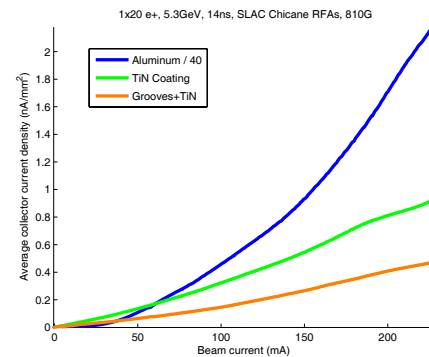


Figure 4: Dipole RFA comparison, 1x20 e+, 14ns, 5.3GeV

azimuthally around the chamber, from about 70 to 150 degrees (taking zero degrees to be the source point). A typical quadrupole RFA measurement is shown in Fig. 5. We find that the collector that is lined up with the quad pole tip (no. 10) sees a large amount of current, while the rest of the collectors see relatively little. This suggests that the majority of the cloud in the quad is streaming between two pole tips.

Fig. 6 shows a comparison of a bare Aluminum (both processed and unprocessed) quadrupole chamber with the TiN coated chamber that has recently replaced it. In this comparison only collector 10 is being plotted. The signal in the TiN chamber was found to be reduced by well over an order of magnitude.

WIGGLER MEASUREMENTS

The L0 straight section of CESR has been reconfigured to include six superconducting wigglers, three of which are instrumented with RFAs [8]. Each wiggler has an RFA in the center of one of the wiggler poles (where the transverse field is largest), half way between poles (where the field is longitudinal), and in an intermediate region. This paper will focus on the center pole RFA, which can roughly be considered to be in a 1.9T dipole field.

Fig. 7 shows a typical Cu wiggler RFA voltage scan for a 45 bunch train of positrons at 1.25mA/bunch, 14ns spacing,

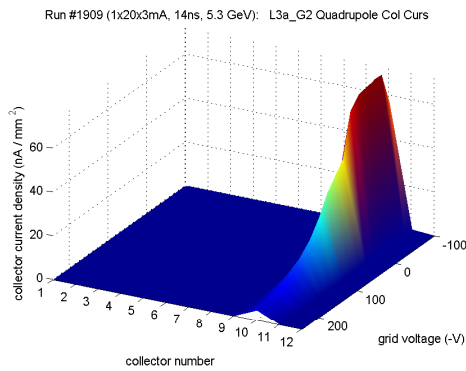


Figure 5: Quadrupole RFA, 1x20x3mA e+, 14ns, 5.3GeV

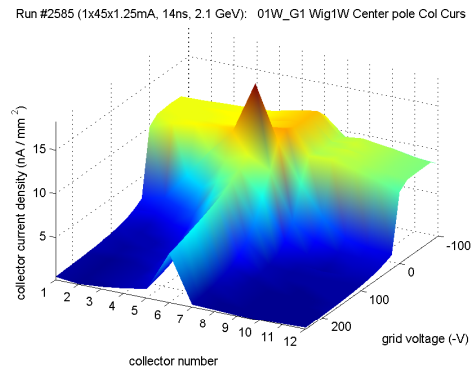


Figure 7: Wiggler RFA measurement, Cu chamber, 1x45x1.25mA e+, 2.1 GeV, 14ns

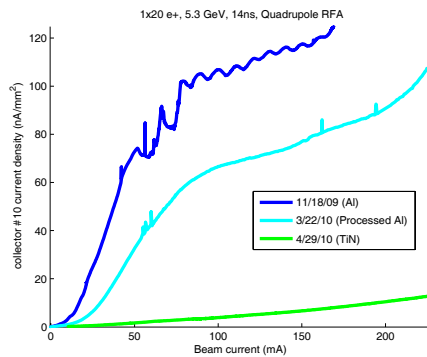


Figure 6: Quad RFA comparison, 1x20 e+, 14ns, 5.3GeV

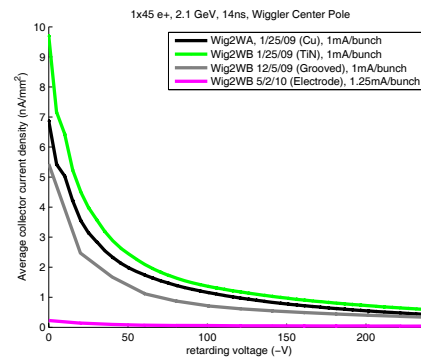


Figure 8: Wiggler comparison, 1x45 e+, 2.1 GeV, 14ns

and 2.1 GeV. The signal is quite constant across all the collectors at low retarding voltage, but does become peaked at the center at high energy. There is also an anomalous spike in current at low (but nonzero) retarding voltage; we believe this is due to a resonance between the bunch spacing and retarding voltage [9].

As with the drift RFAs, cycling the location of the different wigglers has allowed us to compare the RFA response with different mitigation techniques in the same longitudinal position in the ring. We have tested chambers with bare Copper, TiN coating, triangular grooves (with no coating, 2mm depth and 20° angle), and a clearing electrode. Fig. 8 shows the average collector current for a retarding voltage scan in three chambers with mitigation; the copper wiggler is adjacent to this location, and is shown for a rough comparison. Note that, unlike the other measurements presented so far in this paper, beam pipe coating does not appear to lead to a significant reduction in RFA current, and grooves lead only to a small improvement. The chamber instrumented with a clearing electrode, however, shows a sizable reduction in signal. The electrode was set to 400V for this measurement.

CONCLUSIONS

We have found beam pipe coatings (both TiN and Carbon) to be effective at mitigating the cloud in drifts, dipoles,

and quadrupoles. Using a grooved and coated chamber in a dipole is even more effective. In a wiggler, a clearing electrode appears to be the most effective mitigation technique.

These evaluations should all be taken as preliminary. In particular, more work needs to be done to understand the effect of beam processing on these measurements, as well as the details of the wiggler data.

REFERENCES

- [1] E. Shaposhnikova et. al., PAC09, Vancouver, MO6RFP008
- [2] F. Le Pimpec et. al., <http://arxiv.org/abs/physics/0405098v1>
- [3] Y. Suetsugu, H. Fukuma, L. Wang, M. T. F. Pivi, A. Morishige, Y. Suzuki, M. Tsukamoto, NIM-PR-A, 598, 372.
- [4] L. Wang, T. O. Raubenheimer and G. Stupakov, NIM-PR-A, 571, 588 (2007).
M. Pivi, F. K. King, R. E. Kirby, T. O. Raubenheimer, G. Stupakov and F. Le Pmpec, J. Appl. Phys., 104, 104904 (2008).
- [5] M. Palmer et. al., PAC09, Vancouver, TH5RFP030
- [6] R.A. Rosenberg, K.C. Harkay, Nucl. Instrum. Meth. A 453, 507 (2000).
- [7] M. T.F. Pivi, J. S.T. Ng et al. Nucl. Instr. Methods A, doi:10.1016/j.nima.2010.04.052.
- [8] Y. Li et. al., PAC09, Vancouver, TH5RFP029
- [9] J. Calvey et. al., these Proceedings, TUPD022